Title: Merkel Cell Polyomavirus Small Tumor Antigen Activates Matrix Metallopeptidase-9 Gene Expression for Cell Migration and Invasion

Authors

Nnenna Nwogu[1,3], Luz E. Ortiz[1,3], Adrian Whitehouse[2], Hyun Jin Kwun[1,3,*]

Affiliations

[1]Department of Microbiology and Immunology, Penn State University College of Medicine, Hershey, PA, USA

[2]School of Molecular and Cellular Biology and Astbury Centre for Structural Molecular Biology, Faculty of Biological Sciences, University of Leeds, Leeds, United Kingdom.

[3]Penn State Cancer Institute, Hershey, PA, USA

*Correspondence: Hyun Jin Kwun
Department of Microbiology and Immunology, Penn State University College of Medicine, Hershey, PA 17033, USA
E-mail addresses: hxk479@psu.edu
Phone: (717) 512-7241
Fax: (717) 623-7715

Competing interests: The authors declare no competing interests.

Keywords: Merkel cell carcinoma, Merkel cell polyomavirus, small tumor antigen, Matrix Metallopeptidase-9, FBW7, Cell migration, Cell invasion

46 **ABSTRACT**

47 Merkel cell polyomavirus (MCV) small T antigen (sT) is the main oncoprotein for the
48 development of Merkel cell carcinoma (MCC). MCC is a rare, clinically aggressive
49 neuroendocrine tumor of the skin with a high propensity for local, regional, and distant
50 spread. The expression of matrix metalloproteinase (MMP)-9 has been implicated as
51 playing an important role in cell invasion and metastasis in many human cancers.
52 Previously, MCV sT has been shown to increase the cell migration and invasiveness of
53 MCC cells through the transcriptional activation of the sheddase molecule, ADAM 10 (A
54 disintergrin and metalloprotease domain-containing protein 10). In this study, we show
55 that MCV sT protein stimulates epithelial–mesenchymal transition (EMT) gene
56 expression, including MMP-9. This effect is dependent on the presence of the large
57 stabilization domain (LSD), which is known to be responsible for cell transformation
58 through targeting of promiscuous E3 ligases, including FBW7, a known MMP-9
59 regulator. Chemical treatments of MMP-9 markedly inhibited sT-induced cell migration
60 and invasion. These results suggest that sT contributes to the activation of MMP-9 as a
61 result of FBW7 targeting, and increases the invasive potential of cells, which can be
62 used for a targeted therapeutic intervention.

63

64 **IMPORTANCE**

65 Merkel cell carcinoma (MCC) is the most aggressive cutaneous tumor without clearly
66 defined treatment. Although MCC has high propensity for metastasis, little is known about
67 the underlying mechanisms that drive MCC invasion and metastatic progression. MMP-9
68 has shown to play a detrimental role in many metastatic human cancers, including

69 melanoma and other non-melanoma skin cancers. Our study discovers that MCV sT-
70 mediated MMP-9 activation is driven through the LSD, a known E3 ligase targeting
71 domain, in MCC. MMP-9 may serve as the biochemical culprit to target and develop a
72 novel approach for the treatment of metastatic MCC.

INTRODUCTION

Merkel cell carcinoma (MCC) is a rare skin cancer of neuroendocrine origin with a high propensity to metastasize (1). Although the incidence rate of MCC is lower than melanoma, it is highly aggressive with an estimated mortality rate of 33%-46%, hence it is significantly more lethal than malignant melanoma (2). In 90% of cases, it appears in sun-exposed areas of the head, neck and other extremities. This infers that sunlight; specifically, ultraviolet light, plays an important role in MCC development (3, 4). Current epidemiological data highlights the predominance of MCC in elderly patients, inferring that a compromised immune system is an important risk factor in MCC development (5). This is supported by the significantly high incident rates in patient on long-term iatrogenic immunosuppression drugs including organ transplant and HIV/AIDS patients (4). 45% of MCCs reoccur locally, 70% present with early involvement of local lymph nodes, and half result in distant metastases (6). The mortality rate for patients with distant metastases is 80%. This high mortality rate for MCC is due to the highly metastatic nature of the tumor (7).

Merkel cell polyomavirus (MCV) is the etiological agent of MCC. The majority of MCC cases, ~80%, are associated with MCV as observed by monoclonal integration of the MCV genome in the tumor DNA (8). MCV is a common skin commensal, present in ~60% of adults (9). A classic polyomavirus, the genomic organization of MCV is similar to other known human polyomaviruses. MCV expresses small and large tumor antigens (sT and LT), which are essential for viral replication and pathogenesis. MCC derived MCV LT sequences integrated into MCC genomes contain mutations prematurely

97 truncating the helicase domain. These mutations have been shown to render the virus
98 replication-defective and incapable of virus transmission, whilst retaining potentially
99 oncogenic sT and LT coding sequences (10). The LXCXE Retinoblastoma (Rb) protein
100 binding motif in tumor LT remains unaffected in every case, allowing for alteration of cell
101 cycle progression contributing to increased cell proliferation (10).
102
103 MCV sT and truncated LT are essential for MCC cell proliferation and survival. The
104 importance of T antigens have been demonstrated in MCV positive MCC cell lines
105 where small interfering RNA (siRNA)-mediated knockdown of these T antigens induce
106 cell cycle arrest and apoptosis (11). Unlike simian vacuolating virus 40 (SV40), the
107 archetype for polyomavirus studies, both full-length and truncated tumor MCV LT
108 cannot initiate cellular transformation. However, MCV sT is sufficient to induce loss of
109 contact inhibition, anchorage independent, rodent fibroblast transformation and serum
110 independent cell growth (12). As these are hallmarks of an oncogenic viral protein, it
111 can be deduced that MCV sT plays a major role in MCC tumorigenesis.
112
113 MCV sT has been shown to mediate multiple mechanisms which contribute to MCC
114 development. MCV sT induces centrosome overduplication, aneuploidy and micronuclei
115 formation by targeting cellular E3 ligases (13). sT also inhibits SCF^{Fwb7}-mediated
116 degradation of MCV LT and several cellular oncoproteins (14, 15). This is due to the LT
117 stabilizing domain (LSD), a unique domain of sT, binding to SCF E3 ligases (13, 14).
118 Although the exact mechanism by which sT targets E3 ligases is yet to be elucidated, it
119 is clear that the MCV sT LSD plays a major role in the distinctive transforming activities

120 induced by sT (14). MCV sT oncogenic functions induce microtubule destabilization (16)
121 and actin rearrangement (17), which in turn, stimulates cell motility. MCV sT has also
122 been shown to stimulate cell motility by upregulating a disintegrin and metalloproteinase
123 domain-containing protein 10 (ADAM 10) (18).
124
125 FBW7 is an evolutionarily conserved substrate receptor of SCF (complex of SKP1,
126 CUL1 and F-box protein)-type ubiquitin ligases and mediates various proteins that play
127 vital roles in cell division, cell growth and differentiation (19). Upregulation FBXW7
128 provides critical tumor suppressor activity in human cancers and its expression has
129 been linked to inhibition of metastasis and EMT. In various cancers including renal
130 cancer (20), gastric cancer (21) and hepatocellular carcinoma (22), FBW7 inhibition
131 promotes metastasis and EMT by upregulating matrix metalloproteinase expression,
132 specifically MMP-2, MMP-9, and MMP-13.
133
134 Matrix metalloproteinases (MMPs) are a zinc-dependent family of proteolytic enzymes
135 (23). As endo-metalloproteinases, MMPs cleave non-terminal or internal peptide bonds
136 within a protein. MMPs are classified based on the substrate specificity and categorized
137 as collagenases, gelatinases, stromelysins and membrane-type MMPs (MT-MMPs)
138 (24). Interestingly, MMP-2, -9 and -13 are categorized as collagenases, which play a
139 major role in the degradation of the extracellular matrix (ECM) that is essential for
140 maintaining epithelial structural integrity (20). The ECM is comprised of glycoproteins
141 and proteoglycans, such as Type IV collagen and Laminin and provides a barrier from
142 invasion by tumor cells. Degradation of the ECM by MMPs has been identified as an

143 essential mechanism for the metastasis of malignant cells (25). Specifically MMP-9,
144 functions as a collagenase and a gelatinase, and has been associated to multiple
145 hallmarks of cancer, including but not limited to metastasis, invasion, immunological
146 surveillance and angiogenesis (26).
147
148 MMPs also play various roles in multiple virus-induced tumors, by promoting
149 angiogenesis, matrix degradation and tumor invasion. For instance, human papilloma
150 virus (HPV) E7 induces expression of matrix transmembrane metalloproteinase 1 (MT1-
151 MMP), which is crucial for the degradation of the ECM and activation of additional MMP-
152 2 and MMP-9 (27). Hepatitis B and C oncoproteins, HBX and NS5A, both stimulate
153 MMP upregulation which in turn mediates neovascularization as a result of basement
154 membrane degradation (28).
155
156 Tissue invasion is a key component in the process of metastasis and in order to
157 facilitate invasion, the ECM is degraded by MMPs (29). Although there are a variety of
158 MMPs which are essential for tissue development and homeostasis, dysregulation of
159 these proteases has been observed in multiple pathologies, especially in cancers where
160 overexpression of MMPs contribute to tumor progression and tumorigenesis by
161 impinging on multiple mechanisms including but not limited to angiogenesis, cell growth
162 and modulation of migration (24, 30). In the context of virus-induced pathologies, MMPs
163 regulate the final stages of cancer progression in cancer models. Specifically, in a
164 MMTV-polyomavirus middle T-antigen (mice transgenic for the polyomavirus middle T
165 antigen under the control of the mouse mammary tumor virus promoter/enhancer),

166 knockout of MMP-9 resulted in an 80% decrease in lung metastatic burden, signifying
167 the essential role of MMP-9 in angiogenesis and metastasis in this model (31).
168
169 Correlations exist between expression of MMP-9 and various factors associated with
170 tumor progression, implying that MMP-9 is essential for cancer development and the
171 dissemination of metastatic tumor cells (32). Interestingly, when predicting patient
172 outcome, high baseline MMP-9 is associated with poor overall survival (33). As such,
173 there is a current resurgence in research focused on the use of MMP inhibitors. With
174 improved strategies for targeting MMPs, recent studies have shown favorable anti-
175 tumorigenic phenotypes in *in vitro* and *in vivo* studies, which have progressed to clinical
176 trials (34, 35).
177
178 Interrogation of previously published quantitative proteomic datasets of MCV sT-
179 expressing cells demonstrate that MCV sT activates expression of MMP-9 and Snail,
180 known drivers of an epithelial-mesenchymal transition (EMT) and cell migration, whilst
181 sT-downregulated genes relate to cell adhesion molecules. We confirmed both
182 transcriptional and translational regulation of MCV sT activated pleiotropic oncogenic
183 molecules, resulting in induced cell migration in mouse fibroblast cells and human
184 cancer cell lines, including MCV negative MCC in an LSD dependent manner. This
185 indicates that MCV sT targeting of cellular E3 ligases may play a role in sT-induced cell
186 migration and invasion in MCC. Notably, chemical treatment with MMP-9 inhibitors
187 resulted in a dose-dependent reduction in cell migration and invasion. Our results
188 highlight the essential role of MCV-sT LSD in MMP-9 mediated enhanced cell migration

189 and invasion. This suggests that targeting MMP-9 may provide novel therapeutic
190 interventions for disseminated MCC.

191 RESULTS

192 MCV sT expression induces differential expression of proteins associated with
193 EMT.

194 Recent studies have highlighted the involvement of MCV sT in the highly migratory and
195 cell dissociation phenotypes of MCC, elucidating its highly multifunctional roles in MCC
196 (16-18). Previously described SILAC (stable isotope labelling by amino acids in cell
197 culture)-based quantitative proteomics data (REF), was further interrogated to assess
198 the alterations in the host cell proteome upon expression of MCV sT in a HEK293
199 derived cell line (i293-sT) **(Fig. 1A)** (16). These results highlighted an alteration in
200 proteins associated with enhancement of cell migration (microtubule associated
201 cytoskeletal organization) and cell adhesion as previously reported and interestingly the
202 basement membrane, a specialized form of the ECM. Specifically, the quantitative
203 proteomic analysis, showed an almost two-fold decrease in Collagen alpha-2(IV) chain
204 (COL42A) and Laminin subunit gamma-1(LAMC1), two key components of the
205 basement membrane. The basement membrane is essential for epithelial structural
206 integrity. It is comprised of a network of glycoproteins and proteoglycans, such as Type
207 IV collagen and Laminin and provides a barrier from invasion by tumor cells. Therefore,
208 these results suggest that for MCV sT-related oncogenic functions in MCC, the
209 basement membrane must be degraded in order for invasion of tumor cells into the
210 circulatory system for metastasis to occur (37). Aligned with these observations,

211 transcriptome analysis has suggested that certain markers associated with EMT are
212 increased upon MCV-sT expression (38).
213
214 Validation of potential EMT-related markers was performed by qRT-PCR as changes in
215 RNA levels regulate EMT progression due to differential splicing and regulation of EMT
216 markers by microRNAs (39). Classic EMT markers were assessed in MCC13
217 transfected cells and upon MCV-sT expression, a significant downregulation in epithelial
218 markers E-cadherin, ZO-1 and Occludins were observed **(Fig. 1B)**. Conversely,
219 mesenchymal markers ZEB1, ZEB2, Snail, Slug, MMP-3 and MMP-9 were upregulated
220 upon MCV-sT expression. These results infer the possibility of MCV sT inducing an
221 EMT which contributes to the metastatic potential of MCV-associated MCC.
222
223 **MCV sT inhibition of FBW7 contributes to migratory phenotype.**
224 Given the current interest in the role of MCV sT in mediating MCC tumorigenesis,
225 quantifying the migratory capacity of MCC cells, and understanding how the migratory
226 and metastatic capacity may be altered by MCV sT targeting FBW7 was of particular
227 interest. To determine whether sT targeting of FBW7 contributed to sT induced
228 migratory phenotype, a scratch assay was performed comparing vector control, MCV
229 sT_{WT}, and MCV sT_{LSDm} (mutation of the LSD by alanine substitution to inhibit FBW7
230 binding) (36) in transfected U2OS cells. Cellular growth back was recorded and after 24
231 h post scratch, in contrast to vector cells, MCV sT enhanced the motility and migration
232 of cells, consistent with previous studies **(Fig. 2A)**. (16-18, 40, 41). Interestingly, sT
233 mutant, sT_{LSDm}, showed a decrease in sT-induced cell migration. A similar trend was

234 also observed in NIH3T3 mouse fibroblast **(Fig. 2B)** and MCC13 (MCV negative MCC
235 cell line) **(Fig. S1)** expressing vector control, sT_{WT}, and sT_{LSDm}. Enhancement cell
236 migration was readily detected in sT_{WT} but not in sT_{LSDm}, suggesting that inhibiting sT
237 binding of FBW7 was sufficient to repress the MCV sT-induced cell migratory
238 phenotype. H-RasV12 served as a positive control for NIH3T3 transwell assay **(Fig.**
239 **2B)**.
240
241 **MCV sT inhibition of FBW7 prevents turnover of MMP-9.**
242 FBW7 is directly involved in MMP-2, -9 and -13 mediated migration and invasion as a
243 result of regulating expression of these metalloproteases (42). To determine if MMP-9
244 expression contributed to sT induced cell migration, initial assessments to validate
245 whether MCV sT induces MMP-9 expression was performed. A variety of cell lines, 293,
246 COS-9, MCC13 and U2OS cells were transfected with a vector control and MCV sT.
247 MMP-9 gene expression is primarily regulated transcriptionally thereby resulting in low
248 basal levels of these proteases in normal physiology (43). RT-qPCR results showed that
249 MCV sT expression, significantly increased MMP-9 expression in all cell lines tested
250 (**Fig 3A**).
251
252 Previous studies have showed that mutation of the LSD supports turnover of FBW7
253 substrates including LT, Cyclin E and c-Myc (14). It was essential therefore to determine
254 if MCV-sT enhances the migratory potential of MCC by LSD targeting of FBW7 which
255 prevents MMP-9 turnover. Transcriptional and protein levels of MMP-9 were assessed
256 in the presence of the MCV sT_{WT} or MCV sT_{LSDm}. MCV sT-induced upregulation of

257 MMP-9 transcripts was not observed upon mutation of the LSD (**Fig 3B**). Therefore, cell
258 lysates of vector control, MCV sT_{WT} and MCV sT_{LSDm} transfected U2OS and MCC13
259 cells were analyzed to detect MMP-9 by immunoblotting. Our results demonstrated a
260 significant increase in MMP-9 mature protein levels upon MCV sT expression. However,
261 mutation of the LSD prevented MCV sT-mediated upregulation of MMP-9 as expression
262 levels remained comparable with the control, suggesting that MCV sT-mediated
263 upregulation of MMP-9 is LSD dependent (**Fig 3C and 2D**). Studies have shown MMP-
264 9 exists in several forms; a monomeric pro form (~92 kDa), a disulfide-bonded
265 homodimeric (~220 kDa) form and multiple active forms (~67 and 82 kDa) (44, 45). The
266 active and dimeric forms of MMP-9 play a role in the invasive and migratory phenotypes
267 of cancer cells (42, 44, 46). MCV sT_{WT} expression induced upregulation of dimer, pro
268 and active forms of MMP-9, while MMP-9 protein levels upon MCV sT_{LSDm} expression
269 were comparable to vector control confirming that MCV sT upregulation of MMP-9 is
270 LSD dependent.
271
272 **MMP-9 inhibition impedes MCV sT-induced cell migration.**
273 Increased cell migration is associated in various pathological conditions including but
274 not limited to inflammation, rheumatoid arthritis, focal brain ischemia and cancer.
275 Interestingly, increased expression of MMP-9 has been linked to these diseases (47).
276 Consequently, we next assessed if MMP-9 inhibition has an impact in MCV sT induced
277 motile and migratory potentials. The migratory phenotype of U2OS cells transfected with
278 either vector control, MCV sT_{WT} and MCV sT_{LSDm} were assessed using a scratch assay,
279 in the absence or presence of non-cytotoxic concentrations of the MMP9-I and MMP9-II

280 inhibitors (**Fig. S2A**). Incubation of the both inhibitors showed a slight decrease in the
281 motility of vector control cells, implying that any changes observed in migratory rates of
282 MCV sT expression cells is not due to changes in cell viability or cytotoxicity. In
283 contrast, MMP-9 inhibition resulted in a significant decrease in the distance travelled of
284 MCV sT expressing cells (**Fig. 4A and 4B**). Notably, mutation of the LSD impedes sT-
285 induced migration which was further inhibited by MMP-9 inhibition to a degree
286 reminiscent to control cells.
287
288 **MMP-9 is essential for cell motility and migration in MCC.**
289 To demonstrate that MMP-9 is essential for cell motility and migration of MCV-positive
290 MCC cell lines, a transwell migration assay was performed. This assay examines the
291 migration of cells towards a chemoattractant across a permeable chamber. MCV-
292 positive MCC cell lines, MS-1 and MKL-1 were incubated in the absence or presence of
293 the MMP9-I and MMP9-II inhibitors at non-toxic concentrations (**Fig. S2B, C**). After
294 treatment, cells were allowed to migrate for 48 h, cell migration was assessed by cell
295 counting using a cell counting Kit-8 assay. Results showed that migration of MCV-
296 positive MCC cell lines were significantly reduced compared to control, upon treatment
297 with MMP-9 inhibitors suggesting that MMP-9 expression contributes to MCV-Positive
298 MCC cell line migration (**Fig. 4C**). Together, these results suggest that MMP-9 is
299 required for MCV-sT mediated cell migration enhancement in MCC.
300
301 **MCV sT invasive phenotype is LSD dependent.**

302 The invasiveness of epithelial cancers is a multi-step process and a key hallmark
303 involves the degradation of the basement membrane. Type IV collagen is a major
304 component in most basement membranes. Multiple studies have correlated
305 overexpression of MMPs with not only an enhancement of cell migration and
306 metastasis, but also the invasiveness of cancer cells (26, 30, 48). In particular, MMP-9
307 is a key protease associated with the degradation of ECM components including type IV
308 collagen and Laminin which in turn, facilitates invasion of tumors into the circulatory
309 system and promote metastasis. To test if enzymatic activation of MMP-9 is regulated
310 by LSD, we evaluated the MMP-9 substrate, Collagen IV, by immunofluorescence
311 staining. Our results demonstrate that Collagen IV expression in MCV sT_{WT} expressing
312 cells is significantly reduced in comparison to vector control cells. In contrast, MCV-
313 sT_{LSDm} expressing cells did not show a decrease in collagen IV expression (**Fig. 5A**).
314 Moreover, regression analysis revealed that Collagen IV expression levels highly
315 correlated with MCV sT_{WT} or sT_{LSDm} expression levels (**Fig. 5B**).
316
317 To validate the role of the LSD in the invasive phenotype previously observed upon
318 MCV sT expression (16), a collagen invasion assay was performed using collagen
319 precoated inserts in U2OS and MCC13 cells transfected with vector control, MCV sT_{WT}
320 and MCV sT_{LSDm}. Upon mutation of the LSD, MCV sT invasive phenotype was
321 significantly reduced to levels similar to the vector control (**Fig. 5C**), inferring that MCV
322 sT-induced MCC invasion is LSD dependent. Positive expression MCV sT_{WT} and MCV
323 sT_{LSDm} was validated by immunoblotting.
324

325 **MCV sT LSD mediates expression of EMT regulator Snail.**

326 A positive regulatory loop has been identified between MMP-9 and Snail. siRNA
327 mediated inhibition of MMP-9 significantly reduces expression of Snail, and conversely,
328 knockdown of Snail, a transcription factor of MMP-9 also suppressed expression of
329 MMP-9 (49). Moreover, emerging evidence has shown that cellular E3 ligases play a
330 crucial role in the regulation of Snail-mediated EMT (50). In human non-small cell lung
331 cancer, FBW7 inhibited cell migration and invasion due to ubiquitination and proteolytic
332 degradation of Snail while FBW7 silencing induced Snail-mediated EMT in vivo (51).
333 Since Snail is a key initiator of EMT, it was essential to assess the transcriptional and
334 protein levels of Snail in the presence of the MCV sT_{WT} or MCV sT_{LSDm}. RT-qPCR
335 results showed that MCV sT upregulated Snail mRNA levels that was not observed
336 upon mutation of the LSD in U2OS cells (**Fig. 6A)**. Additionally, lysates of vector control,
337 MCV sT_{WT} and MCV sT_{LSDm} transfected U2OS cells were analyzed by immunoblotting
338 for Snail protein expression. Similar to RT-qPCR and SILAC data, our results
339 demonstrated a significant increase in Snail protein levels upon MCV-sT expression that
340 was not observed in MCV sT_{LSDm} expressing cells (**Fig. 6B)**. These data suggest that
341 the LSD possibly impedes FBW7 inhibition of EMT.

342

343 **DISCUSSION**

344 Metastasis is the end point of a series of biological processes by which a tumor cell
345 detaches from the primary tumor and disseminates to a distant site through the
346 circulatory system and establishes a secondary tumor (52). The invasion-metastasis
347 cascade is a multistep process and it has been hypothesized that EMT and

348 mesenchymal-to-epithelial transition (MET) drive the invasion-metastasis cascade
349 (53). Various studies have shown that that oncovirus-associated oncoproteins play a
350 role in metastasis and EMT-related mechanisms. Hepatitis B oncoprotein, HBx, induces
351 MMP-9 through ERK and PI-3K/AKT pathway activation (54). HPV16 E6 and E7
352 oncoproteins have been shown to repress expression of the E-cadherin protein in
353 cervical cancer cells, inducing FGF ligand stimulation resulting in increased
354 invasiveness (38). EBV oncoprotein, LMP1, induces cadherin switching (55) and
355 regulates transcription factors such as TWIST and Snail thereby increasing a migratory
356 phenotype in virus-induced human cancers (56, 57). These cellular targets regulating
357 cancer cell migration and invasion are commonly induced by viral oncoproteins that
358 could be exploited for therapeutic strategies in virus-induced metastatic cancers.
359
360 Cleavage of the ECM allows for creation of space within the extracellular matrix freeing
361 up the surrounding areas for cell migration (58). In this report, we show that MCV sT
362 LSD inhibition of FBW7 potentially promotes upregulation of MMP-9 and contributes to
363 MCV sT-mediated cell migration and invasion. The mechanism by which the LSD
364 inhibition of FBW7 regulates MMP-9 expression is currently unclear, although many
365 studies have shown MMP-9 expression is transcriptionally regulated (24). MMP-9 is
366 also a downstream target of Notch1. It has been demonstrated that loss of FBW7
367 induces Notch1 and Notch1 downstream molecules (MMP-2 and MMP-9) activation,
368 resulting in induced-cell migration and invasion in hepatocellular carcinoma (HCC) (22).
369 Similar trends have been observed in breast cancer where Notch1 signaling promotes
370 an invasive phenotype as a result of activation of NF-κB and its downstream target

371 genes including MMP-2, MMP-9 (59), while downregulation of Notch-1 decreases MMP-
372 9 transcription and function (60). Nonetheless, it is clear that MCV sT LSD plays a
373 critical role in regulating transcriptional and post-translational MMP-9 expression and
374 activity.
375

376 EMT progression is also associated with upregulation of MMPs and cytoskeletal
377 reorganization. Together, both mechanisms enable cell migration and invasion across
378 the basement membrane (61). Additionally, MMPs are also known to target
379 transmembrane proteins, like E-cadherin, contributing to the destabilization of adherens
380 junction. Furthermore, another pathway by which MMPs contribute to EMT is inducing
381 expression of RAC1B, a splice variant of RAC1, which results in upregulation of cellular
382 reactive oxygen species. This in turn induces an increase in Snail expression, which we
383 observed to be upregulated in an LSD dependent manner (**Fig. 6**).

384

385 FBW7 functions as tumor suppressor by negatively regulating oncoproteins in a variety
386 of human cancers and these oncoproteins are degraded by ubiquitination. Studies have
387 shown that FBW7 is a negative regulator of EMT (62, 63). β-TrCP, another key E3
388 ligase that MCV sT targets through the LSD, has been shown to interact with Snail. Two
389 phosphorylation motifs of glycogen synthase kinase-3β (GSK-3β) have been identified
390 in Snail and GSK-3β phosphorylation at motif 1 results in the association of Snail
391 interaction with β-TrCP which induces the ubiquitination and degradation of Snail (64).
392 Furthermore, in MDCK-Snail cells, siRNA depletion of Snail triggered a full reversal to

393 the epithelial phenotype denoted by re-expression key epithelial marker E-cadherin and
394 downregulation mesenchymal markers vimentin and fibronectin, resulting in loss of
395 invasiveness (65). Therefore, we infer that the dysregulation E3 ligases function by
396 MCV sT LSD promotes the metastatic phenotype observed in MCC and inhibition of the
397 LSD-FBW7 interaction could prove to be a novel therapeutic target to reverse the
398 metastatic phenotype observed in MCC.

399

400 The role of MMPs in cancer have been well established and for many years,
401 development of MMP-9 inhibitors focused targeting its active site. Although results from
402 early animal studies utilizing broad spectrum inhibitors were compelling, it was
403 determined that inhibiting such a broad scale inhibition of MMPs interfered with normal
404 tissue function, which could support disease progression (66, 67). Moreover, MMP-9
405 active site inhibitors were prone to off target binding which induced unexpected
406 malignancies including musculoskeletal toxicity (68).

407 Because of the rare and aggressive nature of metastatic MCC and the lack of standard
408 chemotherapy, there are no prospective studies of outcomes following treatment of
409 distant metastatic MCC. The underlying mechanism for the high propensity of MCC
410 tumors to metastasize is yet to be elucidated. MCV-sT has emerged as the main
411 transforming factor significant in both early and late stages of MCV-positive MCC
412 progression. We found that MCV sT specifically activates the EMT-related cellular
413 proteins including MMP-9 through the LSD and can be targeted by commercially available
414 inhibitors, which can be used as second-line treatment for distant metastatic MCC. Our

415 study is the first approach to investigate the therapeutic potential of matrix
416 metalloproteinases in MCC. Standard chemotherapy regimens for metastatic MCC
417 include carboplatin or cisplatin with etoposide and topotecan (69). Because recent FDA
418 approvals of Avelumab and Pembrolizumab represent the only approved treatment option
419 for metastatic MCC (70, 71), it is necessary to evaluate and develop the preclinical activity
420 of efficient and economical chemotherapeutics through retrospective analysis for both
421 MCV-negative and positive MCC patients. MCV-negative MCC tumors patients are more
422 likely to present with advanced disease than patients with virus-positive tumors (66.7%
423 vs. 48.3%) (72), signaling pathways implicated in regulating tumor invasion could be an
424 effective common target for both types of metastatic MCC treatment.

425

426 MATERIAL AND METHODS

427 **Cells.** 293, U2OS and COS-7 cells were maintained in Dulbecco's modified Eagle's
428 medium (DMEM) containing 10% fetal bovine serum (FBS). MCC13, MS-1, MKL-1 and
429 MKL-2 cell lines were maintained in RPMI 1640 medium supplemented with 10% FBS
430 (Seradigm). NIH3T3 cells were maintained in DMEM with 10% bovine calf serum
431 (Seradigm).

432

433 **Plasmids and transfection.** Plasmids for Vector control, codon-optimized cDNA
434 constructs for sT_{WT} and sT_{LSDm} have been previously described (36). For sT protein
435 expression, cells were transfected using Lipofectamine 3000 (Invitrogen) according to the
436 manufacturer's protocol. For lentiviral transduction, codon-optimized cDNAs for MCV sT

437 and H-RasV12 was inserted into pLVX empty vector (36). Plasmids used for this study
438 were listed in **Table S1**.
439
440 **Lentiviral infection.** For lentivirus production, 293FT (Invitrogen) cells were used for
441 induction according to the manufacturer's instructions. NIH3T3 cells were transduced
442 with pLVX empty vector, wild-type or mutant small T antigens lentivirus. Cells were
443 selected with puromycin (3 μg/ml) after infection for one week.
444
445 **Reverse transcription-quantitative polymerase chain reaction (RT-qPCR).** RNA
446 was extracted using Monarch Total RNA miniprep kit (New England Biolabs), as per the
447 manufacturer's instruction. 250 ng of RNA was used as a template in iTaq Universal
448 One-Step RT-qPCR Kits (Bio-Rad) or Luna Universal One-Step RT-qPCR Kit (New
449 England Biolabs) according to the manufacturer's protocol. Primer sequences used are
450 described in **Table S2**. With GAPDH as internal control mRNA, quantitative analysis
451 was performed using the comparative ΔΔCt method.
452
453 **Quantitative immunoblotting (IB) and antibodies.** Cells were lysed in IP buffer (50
454 mM Tris-HCl (pH 8.0), 150 mM NaCl, 1% TritonX-100, 1 mM PMSF, 1 mM
455 benzamidine) and sonicated whole cell lysates were used for direct immunoblotting.
456 Primary antibodies were incubated overnight at 4°C, followed by 1 h secondary antibody
457 incubation at RT. All signals were detected using quantitative Infrared (IR) secondary
458 antibodies (IRDye 800CW goat anti-mouse, 800CW goat anti-rabbit, 680LT goat anti-
459 rabbit IgG, 680LT goat anti-mouse IgG) (LI-COR). Signal intensities were analyzed

460 using a laser-scanning imaging system, Odyssey CLX (LI-COR). Antibodies used for
461 this study were listed in **Table S3**. Protein levels were quantitated and normalized by
462 control, α-tubulin, using an Odyssey LI-COR IR imaging system.
463
464 **SILAC data analysis.** The previously published SILAC-based quantitative proteomic
465 data set analyzing host cell proteome changes upon MCV sT expression (REF) was
466 further interrogated using the Database for Annotation, Visualization and Integrated
467 Discovery (DAVID) v6.7 (51). For quantitative analysis, a 2.0-fold cutoff was chosen as
468 a basis for investigating potential proteome changes (50).
469
470 **Scratch wound-healing assay.** Poly-L-Lysine-coated 6-well plates were seeded with
471 U2OS cells and transfected with either a vector control, MCV sT_{WT} and MCV sT_{LSDm}
472 plasmids. After 48 h, a scratch was created by scraping the monolayer using a p1000
473 pipette tip. Migration of cells toward the scratch was observed over a 24-h period, and
474 images were taken every 8 h under a REVOLVE4 fluorescent microscope (Echo
475 Laboratories). Inhibitor-based scratch assays were incubated for 24 h prior to transfection
476 with 0.1 and 1 μM of 9-I and 9-II inhibitors respectively.
477
478 **Transwell cell migration assay.** Cells grown in DMEM with 10% FBS were trypsinized
479 and resuspended in DMEM. 1×10^5 cells were gently added to the upper compartment
480 of transwell (8 μm, Greiner Bio-One). DMEM with 10% FBS were added to the lower
481 compartment of transwell. The cells were incubated in the culture incubator at 37 °C
482 plus 5% CO2 for indicated time. The remained cells on the upper side were gently
483 removed with cotton balls. The cells migrated from the upper side to the lower side

484 through the filter were fixed with 4% paraformaldehyde in PBS for 10 min, then stained
485 with 1% Crystal Violet in 2% ethanol for 20 min for NIH3T3 cells or cells were counted
486 using a Cell Counting Kit-8 (CCK-8) (Sigma-Aldrich). The stained cells on the lower side
487 were counted under microscope from 5 different randomly selected views. All conditions
488 were the same for assays performed in triplicate.
489
490 **Immunofluorescence.** U2OS cells grown on glass coverslips were transfected with
491 empty vector or sT wild type and LSD mutant expression constructs. After 48 h, cells
492 were then fixed and permeabilized in 1:1 methanol/acetone at -20°C, and blocked in
493 PBS-10% FBS for 1 h. Cells were labeled with the appropriate primary antibodies and
494 then incubated with the appropriate Alexa Fluor-conjugated secondary antibody. Cells
495 were viewed under a REVOLVE4 fluorescent microscope (Echo Laboratories).
496
497 **Collagen invasion assay.** U2OS and MCC13 cells were transfected with sT and LSD
498 mutant expression constructs, allowed to recover for 48 h which was followed by an
499 overnight serum starvation. 1 x10$^{\wedge 6}$ cells in each condition were grown in 24-well cell
500 invasion plate were plated in the top chamber with polymerized collagen-coated
501 membrane (24-well insert; pore size, 8 µm; Chemicon ECM551) in serum free.
502 Complete medium was used as a chemoattractant in the lower chamber. The cells were
503 left to incubate for 72 h, and unattached cells were removed cautiously by cotton swab.
504 Cells that had invaded the lower surface of the membrane were stained with the Cell
505 Stain Solution and counted accordingly. They were finally extracted and detected
506 quantitatively using a standard microplate reader (at 560 nm).

507

508 **Chemical inhibitors.** MMP-9 inhibitors-I and II (EMD Milipore) were used at 0.1 μM
509 and 1 μM, respectively, in U2OS cells lines. In MKL-1 cells, MMP-9 inhibitors-I and II
510 (EMD Milipore) were used at 0.2 μM and 2 μM and in MS-1 cell, 0.1 μM and 1 μM, Cell
511 toxicity was measured using a Cell Counting Kit-8 (CCK-8) (Sigma-Aldrich) according to
512 the manufacturer's protocol.

513

514 **Statistical analysis.** Statistical significance between two groups was determined using
515 one- or two-tailed student's t-tests in either GraphPad Prism (GraphPad Software, Inc.,
516 La Jolla, CA, USA) or Excel. The difference was considered as significant when $p < 0.05$
517 for multiple testing (**Supplemental material**).

518

519 **Acknowledgments**

520 We thank Dr. Patrick S Moore and Dr. Yuan Chang for kind sharing of MCV-related
521 reagents. H.J.K. was supported in part by an Institutional Research Grant, IRG-17-175-
522 04 from the American Cancer Society and by the Pennsylvania Department of Health
523 Tobacco CURE Funds. N.N. was supported by training grant T32 CA060395 from the
524 National Cancer Institute, National Institutes of Health.

525

References

1. Liu W, Yang RF, Payne AS, Schowalter RM, Spurgeon ME, Lambert PF, Xu XW, Buck CB, You JX. 2016. Identifying the Target Cells and Mechanisms of Merkel Cell Polyomavirus Infection. Cell Host & Microbe 19:775-787.
2. Miller RW, Rabkin CS. 1999. Merkel cell carcinoma and melanoma: Etiological similarities and differences (vol 8, pg 153, 1999). Cancer Epidemiology Biomarkers & Prevention 8:485-485.
3. Kaae J, Hansen AV, Biggar RJ, Boyd HA, Moore PS, Wohlfahrt J, Melbye M. 2010. Merkel Cell Carcinoma: Incidence, Mortality, and Risk of Other Cancers. Journal of the National Cancer Institute 102:793-801.
4. Soltani AM, Allan BJ, Best MJ, Panthaki ZJ, Thaller SR. 2014. Merkel cell carcinoma of the hand and upper extremity: Current trends and outcomes. Journal of Plastic Reconstructive and Aesthetic Surgery 67:E71-E77.
5. Heath M, Jaimes N, Lemos B, Mostaghimi A, Wang LC, Penas PE, Nghiem P. 2008. Clinical characteristics of Merkel cell carcinoma at diagnosis in 195 patients: the AEIOU features. Journal of the American Academy of Dermatology 58:375-381.
6. Schadendorf D, Lebbé C, Zur Hausen A, Avril MF, Hariharan S, Bharmal M, Becker JC. 2017. Merkel cell carcinoma: Epidemiology, prognosis, therapy and unmet medical needs. Eur J Cancer 71:53-69.
7. Sarnaik AA, Lien MH, Nghiem P, Bichakjian CK. 2010. Clinical Recognition, Diagnosis, and Staging of Merkel Cell Carcinoma, and the Role of the Multidisciplinary Management Team. Current Problems in Cancer 34:38-46.
8. Feng H, Shuda M, Chang Y, Moore PS. 2008. Clonal integration of a polyomavirus in human Merkel cell carcinoma. Science 319:1096-100.
9. Moore PS, Chang Y. 2017. Common Commensal Cancer Viruses. Plos Pathogens 13:6.
10. Shuda M, Feng H, Kwun HJ, Rosen ST, Gjoerup O, Moore PS, Chang Y. 2008. T antigen mutations are a human tumor-specific signature for Merkel cell polyomavirus. Proc Natl Acad Sci U S A 105:16272-7.
11. Houben R, Shuda M, Schrama D, Chang Y, Moore P, Becker JC. 2010. Merkel cell polyoma virus T antigen induces survivin and is required for the tumor phenoptype of infected Merkel cell carcinoma cells. Experimental Dermatology 19:209-209.
12. Shuda M, Kwun HJ, Feng HC, Chang Y, Moore PS. 2011. Human Merkel cell polyomavirus small T antigen is an oncoprotein targeting the 4E-BP1 translation regulator. Journal of Clinical Investigation 121:3623-3634.
13. Kwun HJ, Wendzicki JA, Shuda Y, Moore PS, Chang Y. 2017. Merkel cell polyomavirus small T antigen induces genome instability by E3 ubiquitin ligase targeting. Oncogene 36:6784-6792.
14. Kwun HJ, Shuda M, Feng H, Camacho CJ, Moore PS, Chang Y. 2013. Merkel Cell Polyomavirus Small T Antigen Controls Viral Replication and Oncoprotein Expression by Targeting the Cellular Ubiquitin Ligase SCFFbw7. Cell Host & Microbe 14:125-135.

571 15. Verhaegen ME, Mangelberger D, Harms PW, Vozheiko TD, Weick JW, Wilbert
572 DM, Saunders TL, Ermilov AN, Bichakjian CK, Johnson TM, Imperiale MJ,
573 Dlugosz AA. 2015. Merkel cell polyomavirus small T antigen is oncogenic in
574 transgenic mice. J Invest Dermatol 135:1415-1424.
575 16. Knight LM, Stakaityte G, Wood JJ, Abdul-Sada H, Griffiths DA, Howell GJ, Wheat
576 R, Blair GE, Steven NM, Macdonald A, Blackbourn DJ, Whitehouse A. 2015.
577 Merkel cell polyomavirus small T antigen mediates microtubule destabilization to
578 promote cell motility and migration. J Virol 89:35-47.
579 17. Stakaityte G, Nwogu N, Dobson SJ, Knight LM, Wasson CW, Salguero FJ,
580 Blackbourn DJ, Blair GE, Mankouri J, Macdonald A, Whitehouse A. 2018. Merkel
581 Cell Polyomavirus Small T Antigen Drives Cell Motility via Rho-GTPase-Induced
582 Filopodium Formation. Journal of Virology 92.
583 18. Nwogu N, Boyne JR, Dobson SJ, Poterlowicz K, Blair GE, Macdonald A,
584 Mankouri J, Whitehouse A. 2018. Cellular sheddases are induced by Merkel cell
585 polyomavirus small tumour antigen to mediate cell dissociation and invasiveness.
586 Plos Pathogens 14.
587 19. Ang XL, Wade Harper J. 2005. SCF-mediated protein degradation and cell cycle
588 control. Oncogene 24:2860-70.
589 20. Sailo BL, Banik K, Girisa S, Bordoloi D, Fan L, Halim CE, Wang H, Kumar AP,
590 Zheng DL, Mao XL, Sethi G, Kunnumakkara AB. 2019. FBXW7 in Cancer: What
591 Has Been Unraveled Thus Far? Cancers 11:31.
592 21. Calcagno DQ, Freitas VM, Leal MF, De Souza CRT, Demachki S, Montenegro R,
593 Assumpcao PP, Khayat AS, Smith MDC, dos Santos A, Burbano RR. 2013.
594 MYC, FBXW7 and TP53 copy number variation and expression in Gastric
595 Cancer. Bmc Gastroenterology 13.
596 22. Wang X, Zhang J, Zhou L, Sun W, Zheng ZG, Lu P, Gao Y, Yang XS, Zhang ZC,
597 Tao KS, Dou KF. 2015. Fbxw7 regulates hepatocellular carcinoma migration and
598 invasion via Notch1 signaling pathway. International Journal of Oncology 47:231-
599 243.
600 23. Loffek S, Schilling O, Franzke CW. 2011. Biological role of matrix
601 metalloproteinases: a critical balance. European Respiratory Journal 38:191-208.
602 24. Nagase H, Woessner JF. 1999. Matrix metalloproteinases. Journal of Biological
603 Chemistry 274:21491-21494.
604 25. Walker C, Mojares E, Hernandez AD. 2018. Role of Extracellular Matrix in
605 Development and Cancer Progression. International Journal of Molecular
606 Sciences 19.
607 26. Huang H. 2018. Matrix Metalloproteinase-9 (MMP-9) as a Cancer Biomarker and
608 MMP-9 Biosensors: Recent Advances. Sensors 18.
609 27. Zhu DJ, Ye M, Zhang W. 2015. E6/E7 oncoproteins of high risk HPV-16
610 upregulate MT1-MMP, MMP-2 and MMP-9 and promote the migration of cervical
611 cancer cells. International Journal of Clinical and Experimental Pathology 8:4981-
612 4989.
613 28. viruses AaohBaC. 2012. Angiogenic Activity of Hepatitis B and C Viruses.
614 Antiviral Chemistry & Chemotherapy 22:11.

615 29. Radisky ES, Radisky DC. 2010. Matrix Metalloproteinase-Induced Epithelial-
616 Mesenchymal Transition in Breast Cancer. Journal of Mammary Gland Biology
617 and Neoplasia 15:201-212.
618 30. Gialeli C, Theocharis AD, Karamanos NK. 2011. Roles of matrix
619 metalloproteinases in cancer progression and their pharmacological targeting.
620 Febs Journal 278:16-27.
621 31. Martin MD, Carter KJ, Jean-Philippe SR, Chang M, Mobashery S, Thiolloy S,
622 Lynch CC, Matrisian LM, Fingleton B. 2008. Effect of ablation or inhibition of
623 stromal matrix metalloproteinase-9 on lung metastasis in a breast cancer model
624 is dependent on genetic background. Cancer Research 68:6251-6259.
625 32. Farina AR, Mackay AR. 2014. Gelatinase B/MMP-9 in Tumour Pathogenesis and
626 Progression. Cancers 6:240-296.
627 33. Tabouret E, Bertucci F, Pierga JY, Petit T, Levy C, Ferrero JM, Campone M,
628 Gligorov J, Lerebours F, Roche H, Bachelot T, van Laere S, Ueno NT, Toiron Y,
629 Finetti P, Birnbaum D, Borg JP, Viens P, Chinot O, Goncalves A. 2016. MMP2
630 and MMP9 serum levels are associated with favorable outcome in patients with
631 inflammatory breast cancer treated with bevacizumab-based neoadjuvant
632 chemotherapy in the BEVERLY-2 study. Oncotarget 7:18531-18540.
633 34. Fields GB. 2019. Mechanisms of Action of Novel Drugs Targeting Angiogenesis-
634 Promoting Matrix Metalloproteinases. Frontiers in Immunology 10.
635 35. Fields GB. 2019. The Rebirth of Matrix Metalloproteinase Inhibitors: Moving
636 Beyond the Dogma. Cells 8.
637 36. Kwun HJ, Shuda M, Feng H, Camacho CJ, Moore PS, Chang Y. 2013. Merkel
638 cell polyomavirus small T antigen controls viral replication and oncoprotein
639 expression by targeting the cellular ubiquitin ligase SCFFbw7. Cell Host Microbe
640 14:125-35.
641 37. Horejs CM. 2016. Basement membrane fragments in the context of the epithelial-
642 to-mesenchymal transition. European Journal of Cell Biology 95:427-440.
643 38. Berrios C, Padi M, Keibler MA, Park DE, Molla V, Cheng JW, Lee SM,
644 Stephanopoulos G, Quackenbush J, DeCaprio JA. 2016. Merkel Cell
645 Polyomavirus Small T Antigen Promotes Pro-Glycolytic Metabolic Perturbations
646 Required for Transformation. Plos Pathogens 12:21.
647 39. Lamouille S, Xu J, Derynck R. 2014. Molecular mechanisms of epithelial-
648 mesenchymal transition. Nature Reviews Molecular Cell Biology 15:178-196.
649 40. Stakaityte G, Wood JJ, Knight LM, Abdul-Sada H, Adzahar NS, Nwogu N,
650 Macdonald A, Whitehouse A. 2014. Merkel Cell Polyomavirus: Molecular Insights
651 into the Most Recently Discovered Human Tumour Virus. Cancers 6:1267-1297.
652 41. Stakaityte G, Nwogu N, Lippiat JD, Blair GE, Poterlowicz K, Boyne JR,
653 Macdonald A, Mankouri J, Whitehouse A. 2018. The cellular chloride channels
654 CLIC1 and CLIC4 contribute to virus-mediated cell motility. Journal of Biological
655 Chemistry 293:4582-4590.
656 42. Cai YK, Zhang M, Qiu XF, Wang BW, Fu Y, Zeng J, Bai J, Yang GS. 2017.
657 Upregulation of FBXW7 Suppresses Renal Cancer Metastasis and Epithelial
658 Mesenchymal Transition. Disease Markers.

659 43. Fanjul-Fernandez M, Folgueras AR, Cabrera S, Lopez-Otin C. 2010. Matrix
660 metalloproteinases: Evolution, gene regulation and functional analysis in mouse
661 models. Biochimica Et Biophysica Acta-Molecular Cell Research 1803:3-19.
662 44. Olson MW, Bernardo MM, Pietila M, Gervasi DC, Toth M, Kotra LP, Massova I,
663 Mobashery S, Fridman R. 2000. Characterization of the monomeric and dimeric
664 forms of latent and active matrix metalloproteinase-9 - Differential rates for
665 activation by stromelysin 1. Journal of Biological Chemistry 275:2661-2668.
666 45. Shimokawa K, Katayama M, Matsuda Y, Takahashi H, Hara I, Sato H, Kaneko S.
667 2002. Matrix metalloproteinase (MMP)-2 and MMP-9 activities in human seminal
668 plasma. Molecular Human Reproduction 8:32-36.
669 46. Dufour A, Zucker S, Sampson NS, Kuscu C, Cao JA. 2010. Role of Matrix
670 Metalloproteinase-9 Dimers in Cell Migration DESIGN OF INHIBITORY
671 PEPTIDES. Journal of Biological Chemistry 285:35944-35956.
672 47. Sternlicht MD, Werb Z. 2001. How matrix metalloproteinases regulate cell
673 behavior. Annual Review of Cell and Developmental Biology 17:463-516.
674 48. Mehner C, Hockla A, Miller E, Ran S, Radisky DC, Radisky ES. 2014. Tumor
675 cell-produced matrix metalloproteinase 9 (MMP-9) drives malignant progression
676 and metastasis of basal-like triple negative breast cancer. Oncotarget 5:2736-
677 2749.
678 49. Lin CY, Tsai PH, Kandaswami CC, Lee PP, Huang CJ, Hwang JJ, Lee MT. 2011.
679 Matrix metalloproteinase-9 cooperates with transcription factor Snail to induce
680 epithelial-mesenchymal transition. Cancer Science 102:815-827.
681 50. Li H, Wang ZW, Zhang W, Qian K, Xu W, Zhang SR. 2016. Fbxw7 regulates
682 tumor apoptosis, growth arrest and the epithelial-to-mesenchymal transition in
683 part through the RhoA signaling pathway in gastric cancer. Cancer Letters
684 370:39-55.
685 51. Zhang Y, Zhang XX, Ye MX, Jing PY, Xiong J, Han ZP, Kong J, Li MY, Lai XF,
686 Chang N, Zhang J. 2018. FBW7 loss promotes epithelial-to-mesenchymal
687 transition in non-small cell lung cancer through the stabilization of Snail protein.
688 Cancer Letters 419:75-83.
689 52. Valastyan S, Weinberg RA. 2011. Tumor Metastasis: Molecular Insights and
690 Evolving Paradigms. Cell 147:275-292.
691 53. Thiery JP. 2002. Epithelial-mesenchymal transitions in tumour progression.
692 Nature Reviews Cancer 2:442-454.
693 54. Chung TW, Lee YC, Kim CH. 2004. Hepatitis B viral HBx induces matrix
694 metalloproteinase-9 gene expression through activation of ERK and PI-3K/AKT
695 pathways: involvement of invasive potential. FASEB J 18:1123-5.
696 55. Shair KHY, Schnegg CI, Raab-Traub N. 2009. Epstein-Barr Virus Latent
697 Membrane Protein-1 Effects on Junctional Plakoglobin and Induction of a
698 Cadherin Switch. Cancer Research 69:5734-5742.
699 56. Horikawa T, Yoshizaki T, Kondo S, Furukawa M, Kaizaki Y, Pagano JS. 2011.
700 Epstein-Barr Virus latent membrane protein 1 induces Snail and epithelial-
701 mesenchymal transition in metastatic nasopharyngeal carcinoma. British Journal
702 of Cancer 104:1160-1167.
703 57. Morris MA, Laverick L, Wei WB, Davis AM, O'Neill S, Wood L, Wright J, Dawson
704 CW, Young LS. 2018. The EBV-Encoded Oncoprotein, LMP1, Induces an

705 Epithelial-to-Mesenchymal Transition (EMT) via Its CTAR1 Domain through
706 Integrin-Mediated ERK-MAPK Signalling. Cancers 10.
707 58. Reinhard J, Joachim SC, Faissner A. 2015. Extracellular matrix remodeling
708 during retinal development. Experimental Eye Research 133:132-140.
709 59. Brzozowa-Zasada M, Piecuch A, Michalski M, Segiet O, Kurek J, Harabin-
710 Slowinska M, Wojnicz R. 2017. Notch and its oncogenic activity in human
711 malignancies. European Surgery-Acta Chirurgica Austriaca 49:199-209.
712 60. Bin Hafeez B, Adhami VM, Asim M, Siddiqui IA, Bhat KM, Zhong WX, Saleem M,
713 Din M, Setaluri V, Mukhtar H. 2009. Targeted Knockdown of Notch1 Inhibits
714 Invasion of Human Prostate Cancer Cells Concomitant with Inhibition of Matrix
715 Metalloproteinase-9 and Urokinase Plasminogen Activator. Clinical Cancer
716 Research 15:452-459.
717 61. Aresu L, Benali S, Garbisa S, Gallo E, Castagnaro M. 2011. Matrix
718 metalloproteinases and their role in the renal epithelial mesenchymal transition.
719 Histology and Histopathology 26:307-313.
720 62. Jiang GB, Shi WW, Fang HY, Zhang XH. 2018. miR-27a promotes human breast
721 cancer cell migration by inducing EMT in a FBXW7-dependent manner.
722 Molecular Medicine Reports 18:5417-5426.
723 63. Li NN, Babaei-Jadidi R, Lorenzi F, Spencer-Dene B, Clarke P, Domingo E,
724 Tulchinsky E, Vries RGJ, Kerr D, Pan YH, He YL, Bates DO, Tomlinson I,
725 Clevers H, Nateri AS. 2019. An FBXW7-ZEB2 axis links EMT and tumour
726 microenvironment to promote colorectal cancer stem cells and chemoresistance.
727 Oncogenesis 8.
728 64. Zhou BHP, Deng J, Xia WY, Xu JH, Li YM, Gunduz M, Hung MC. 2004. Dual
729 regulation of Snail by GSK-3 beta-mediated phosphorylation in control of
730 epithelial-mesenchymal transition. Nature Cell Biology 6:931-+.
731 65. Przybylo JA, Radisky DC. 2007. Matrix metalloproteinase-induced epithelial-
732 mesenchymal transition: Tumor progression at Snail's pace. International Journal
733 of Biochemistry & Cell Biology 39:1082-1088.
734 66. Overall CM, Kleifeld O. 2006. Towards third generation matrix metalloproteinase
735 inhibitors for cancer therapy. British Journal of Cancer 94:941-946.
736 67. Page-McCaw A, Ewald AJ, Werb Z. 2007. Matrix metalloproteinases and the
737 regulation of tissue remodelling. Nature Reviews Molecular Cell Biology 8:221-
738 233.
739 68. Scannevin RH, Alexander R, Haarlander TM, Burke SL, Singer M, Huo CF,
740 Zhang YM, Maguire D, Spurlino J, Deckman I, Carroll KI, Lewandowski F, Devine
741 E, Dzordzorme K, Tounge B, Milligan C, Bayoumy S, Williams R, Schalk-Hihi C,
742 Leonard K, Jackson P, Todd M, Kuo LC, Rhodes KJ. 2017. Discovery of a highly
743 selective chemical inhibitor of matrix metalloproteinase-9 (MMP-9) that
744 allosterically inhibits zymogen activation. Journal of Biological Chemistry
745 292:17963-17974.
746 69. Cowey CL, Mahnke L, Espirito J, Helwig C, Oksen D, Bharmal M. 2017. Real-
747 world treatment outcomes in patients with metastatic Merkel cell carcinoma
748 treated with chemotherapy in the USA. Future Oncology 13:1699-1710.

749 70. Joseph J, Zobniw C, Davis J, Anderson J, Trinh V. 2018. Avelumab: A Review of
750 Its Application in Metastatic Merkel Cell Carcinoma. Annals of Pharmacotherapy
751 52:928-935.
752 71. Shirley M. 2018. Avelumab: A Review in Metastatic Merkel Cell Carcinoma.
753 Targeted Oncology 13:409-416.
754 72. Moshiri AS, Doumani R, Yelistratova L, Blom A, Lachance K, Shinohara MM,
755 Delaney M, Chang O, McArdle S, Thomas H, Asgari MM, Huang ML, Schwartz
756 SM, Nghiem P. 2017. Polyomavirus-Negative Merkel Cell Carcinoma: A More
757 Aggressive Subtype Based on Analysis of 282 Cases Using Multimodal Tumor
758 Virus Detection. Journal of Investigative Dermatology 137:819-827.
759
760
761

762 **FIGURE LEGENDS**

763 **FIGURE 1**

764 **MCV ST expression leads to differential expression of proteins associated with**
765 **epithelial to mesenchymal transition (EMT). (A)** Quantitative proteomics analysis
766 illustrating fold difference of differential expression of EMT associated proteins upon MCV-
767 sT expression. Proteins associated with cell adhesion and structural integrity of the of the
768 extracellular matrix are downregulated upon MCV sT expression. An increase in expression
769 of proteins which encourage cell migration by reorganization of the actin network and
770 microtubule destabilization are upregulated. **(B)** MCC13 cells were transfected with control
771 or MCV sT expression plasmids. Cellular RNA was extracted using a trizol reagent, reverse
772 transcribed and qRT-PCR was performed. Transcript levels were analyzed using the
773 comparative CT method (n = 3).

774 **FIGURE 2**

775 **MCV sT induces cell motility in an LSD dependent manner. (A)** Scratch assay. Poly-
776 L-lysine-coated 6-well plates were seeded with U2OS cells and transfected with either a
777 vector control, MCV sT_{WT} and MCV sT_{LSDm} plasmids. After 48 h, a scratch was created
778 by scraping the monolayer using a p1000 pipette tip. Migration of cells toward the
779 scratch was observed over a 24 h period, and images were taken every 8 h under a
780 REVOLVE4 fluorescent microscope (Echo Laboratories). The size of the wound was
781 measured at 0 and 24 h. Scratch assays were performed in triplicate., n = 3 and
782 differences between means (*p* value) were analyzed using a t-test with GraphPad Prism
783 software. Protein expression levels of MCV sT wild type and mutant samples. Protein
784 expression was detected by immunoblot analysis to validate successful transfection.

785 Quantitative Infrared fluorescence immunoblotting was performed using 2T2 antibody
786 for sT antigens and alpha-tubulin, respectively. Differences between means (*p* value)
787 were analyzed using a t-test with GraphPad Prism software. **(B)** Transwell migration
788 assay**.** NIH3T3 cells stably expressing an empty vector, H-RasV12, MCV sT_{WT} and
789 MCV sT_{LSDm} (Fbw7 binding mutant) were trypsinized and $2x10^5$ cells were seeded into
790 transwell inserts and incubated for 5 days. Images represent wells samples tested. The
791 experiments were performed two times and the results were reproducible. Graph
792 indicates the fold difference of migrated cells relative to the vector control sample.
793 Protein expression was determined by immunoblotting.

794 **FIGURE 3**

795 **Matrix metalloproteinases 9 (MMP-9) activation in MCV sT expressing cells is LSD**
796 **dependent.** (A) Various cell lines (293, COS-7, MCC13 and U2OS) were transfected for
797 48 h with a vector control and MCV sT_{WT} expressing plasmids. (B) U2OS and MCC13
798 cells transfected with empty vector control, MCV sT_{WT} and MCV sT_{LSDm} expressing
799 plasmids. Cellular RNA was extracted and transcript levels were analyzed using the
800 comparative CT method (n = 3). Data analyzed using three replicates per experiment
801 and statistical analysis using a two-tailed t-test with unequal variance comparing MCV
802 sT_{WT} and sT_{LSDm} samples to control samples. Differences between means (*p* value)
803 were analyzed using a t-test with GraphPad Prism software. (C) U2OS cells (D) MCC13
804 Cells were transfected with vector control, and MCV sT_{WT} and MCV sT_{LSDm} expressing
805 plasmids expression plasmids for 48 h. (I) Immunoblot analysis was performed on the
806 cellular lysates and analyzed MMP-9 specific antibody, α-tubulin was used as a

807 measure of equal loading and the 2T2 hybridoma was used to confirm MCV-sT wild
808 type and mutant expression. (II) Densitometry quantification of immunoblots was carried
809 out using the Image studio software and is shown as a fold change relative to the
810 loading control, α-tubulin. Data analyzed using three biological replicates per
811 experiment (n = 3).

812 **FIGURE 4**

813 **MMP-9 inhibition impedes MCV sT-induced cell migration.** (A) Scratch assay. Poly-
814 L-lysine-coated 6-well plates were seeded with U2OS cells and incubated with specific
815 inhibitors at predetermined concentrations. Cells were transfected with either a vector
816 control, MCV sT_{WT} and MCV sT_{LSDm} plasmids. After 48 h, a scratch was created and
817 migration of cells toward the scratch was observed over a 24 h period. The size of the
818 wound was measured at 0 and 24 h. Scratch assays were performed in triplicate. (B)
819 MCV positive MCC cell lines, MKL-1 and MS1, were incubated with DMSO or the MMP-
820 9 inhibitors 9-I (0.2 μM).and -II (2 μM); 9-I (0.1 μM).and -II (1 μM). Cells were then
821 transferred into migration wells and allowed to migrate from serum-free to 10% FBS
822 conditions for 48 h. Migratory cells were incubated CCK-8 solution and measured at 450
823 nm to quantify migration. Data analyzed using three biological replicates per
824 experiment, n = 3. Differences between means (*p* value) were analyzed using a t-test
825 with GraphPad Prism software.

826 **FIGURE 5**

827 **MCV sT LSD induces collagen degradation.** (A) U2OS cells were transfected with
828 empty vector control, MCV sT_{WT} and MCV sT_{LSDm} plasmids. 48 h post transfection, cells

829 were fixed and endogenous Collagen IV levels were identified by indirect
830 immunofluorescence using a specific antibody. MCV sT expression was detected with
831 2T2 T antigen antibody. (B) Mean Florescence intensity of wildtype and mutant MCV sT
832 and Collagen IV expression was analyzed using Fiji Image J software. The calculated
833 values were plotted for regression analysis. (C) Collagen invasion assay. Precoated
834 collagen inserts were seeded with serum starved U2OS transfected cells and incubated
835 for 72 h, then labelled with a cell staining solution for 20 mins. Upon extraction of the
836 cell staining solution, absorbance at OD560 was measured. Data analyzed using three
837 replicates per experiment, the experiments were performed two times. The results were
838 reproducible and differences between means (*p* value) were analyzed using a t-test with
839 GraphPad Prism software. (C) Expression of oncoproteins. Protein expression levels of
840 wild type and mutant MCV sT. Protein expression was detected by immunoblot analysis
841 to validate successful transfection. Quantitative infrared fluorescence immunoblotting
842 was performed using 2T2 antibody for sT antigens and α-tubulin, respectively.

843 **FIGURE 6**

844 **MCV sT LSD induces Snail expression.** (A) U2OS cells were transfected with empty
845 vector control, MCV sT_{WT} and MCV sT_{LSDm} expressing plasmids. Cellular RNA was
846 extracted at 48 h post transfection and transcript levels were analyzed using the
847 comparative CT method (n = 3). (B) Snail expression is induced by sT. Immunoblot
848 analysis was performed on the cellular lysates and analyzed using Snail specific
849 antibody. α-tubulin was used as a measure of equal loading and the 2T2 antibody was
850 used to confirm MCV sT wild type and mutant expression.
851

FIG 1

A

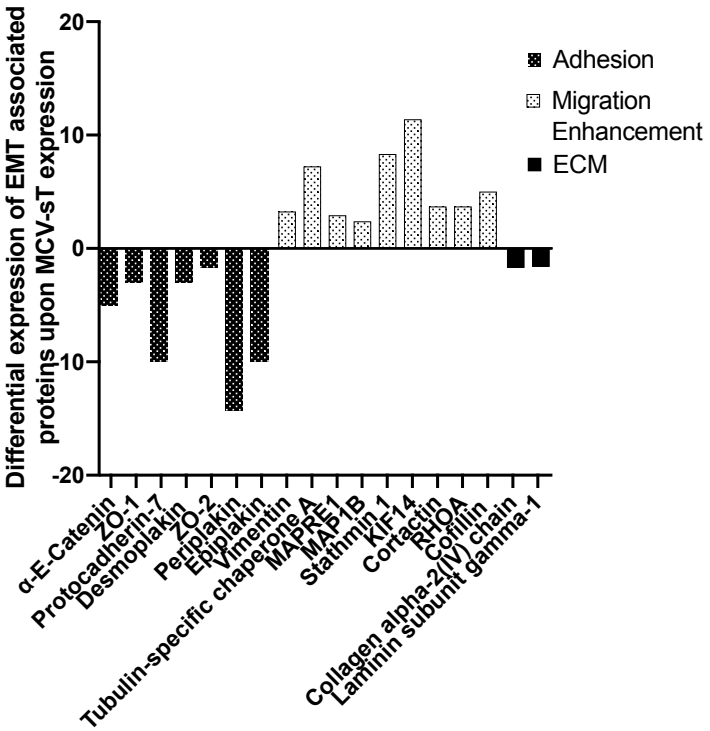
Differential expression of EMT associated proteins upon MCV-sT expression
20
10
0
-10
-20
Adhesion
Migration Enhancement
ECM
α-E-Catenin
ZO-1
Protocadherin-7
Desmoplakin
ZO-2
Periplakin
Epiplakin
Vimentin
Tubulin-specific chaperone A
MAPRE1
MAP1B
Stathmin 1
KIF14
Cortactin
RHOA
Cofilin
Collagen alpha-2(IV) chain
Laminin subunit gamma-1

B

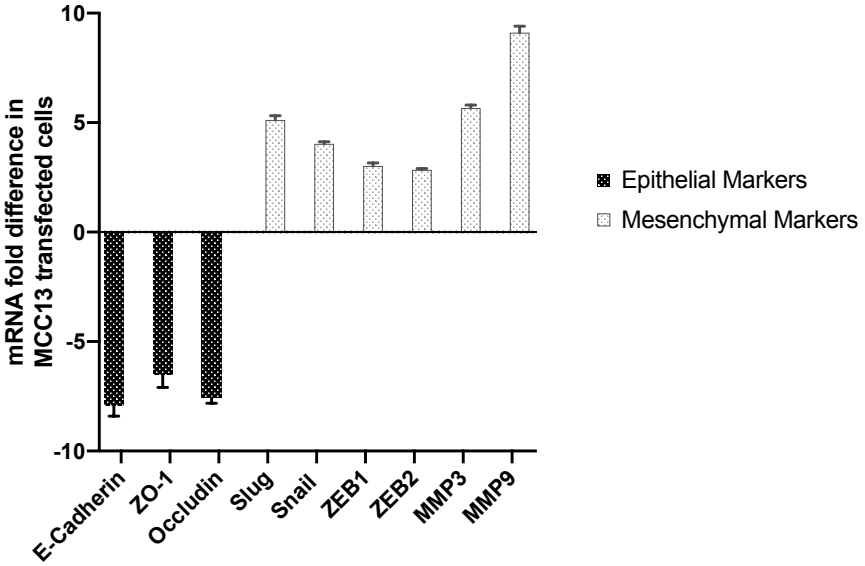
mRNA fold difference in MCC13 transfected cells
10
5
0
-5
-10
Epithelial Markers
Mesenchymal Markers
E-Cadherin
ZO-1
Occludin
Slug
Snail
ZEB1
ZEB2
MMP3
MMP9

FIG 2

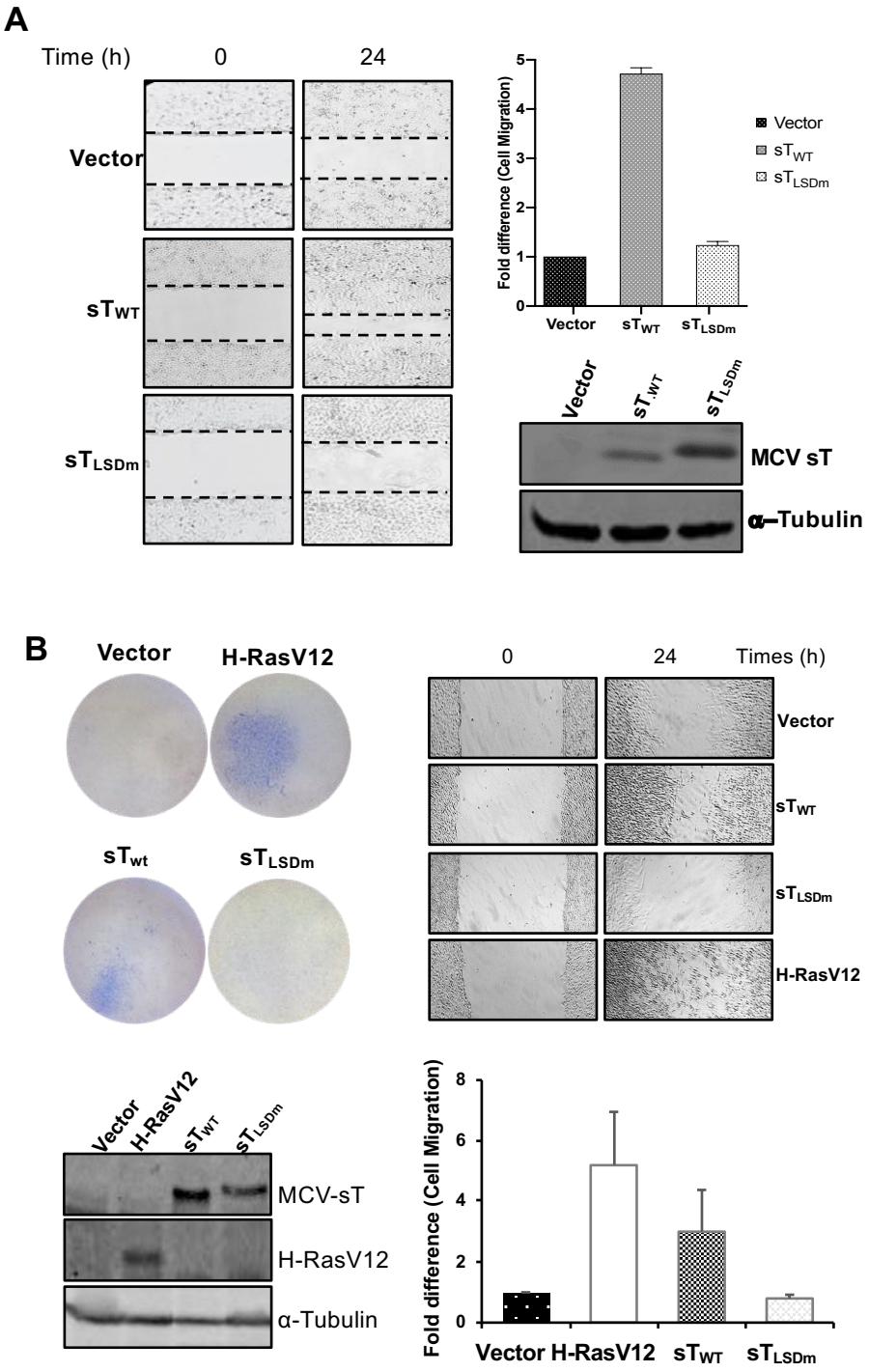
A
Time (h)
0
24
Vector
sTWT
sTLSDm
Fold difference (Cell Migration)
Vector
sTWT
sTLSDm
MCV sT
α–Tubulin
B
Vector
H-RasV12
sTwt
sTLSDm
0
24
Times (h)
Vector
sTWT
sTLSDm
H-RasV12
MCV-sT
H-RasV12
α-Tubulin
Fold difference (Cell Migration)
Vector
H-RasV12
sTWT
sTLSDm

FIG 3

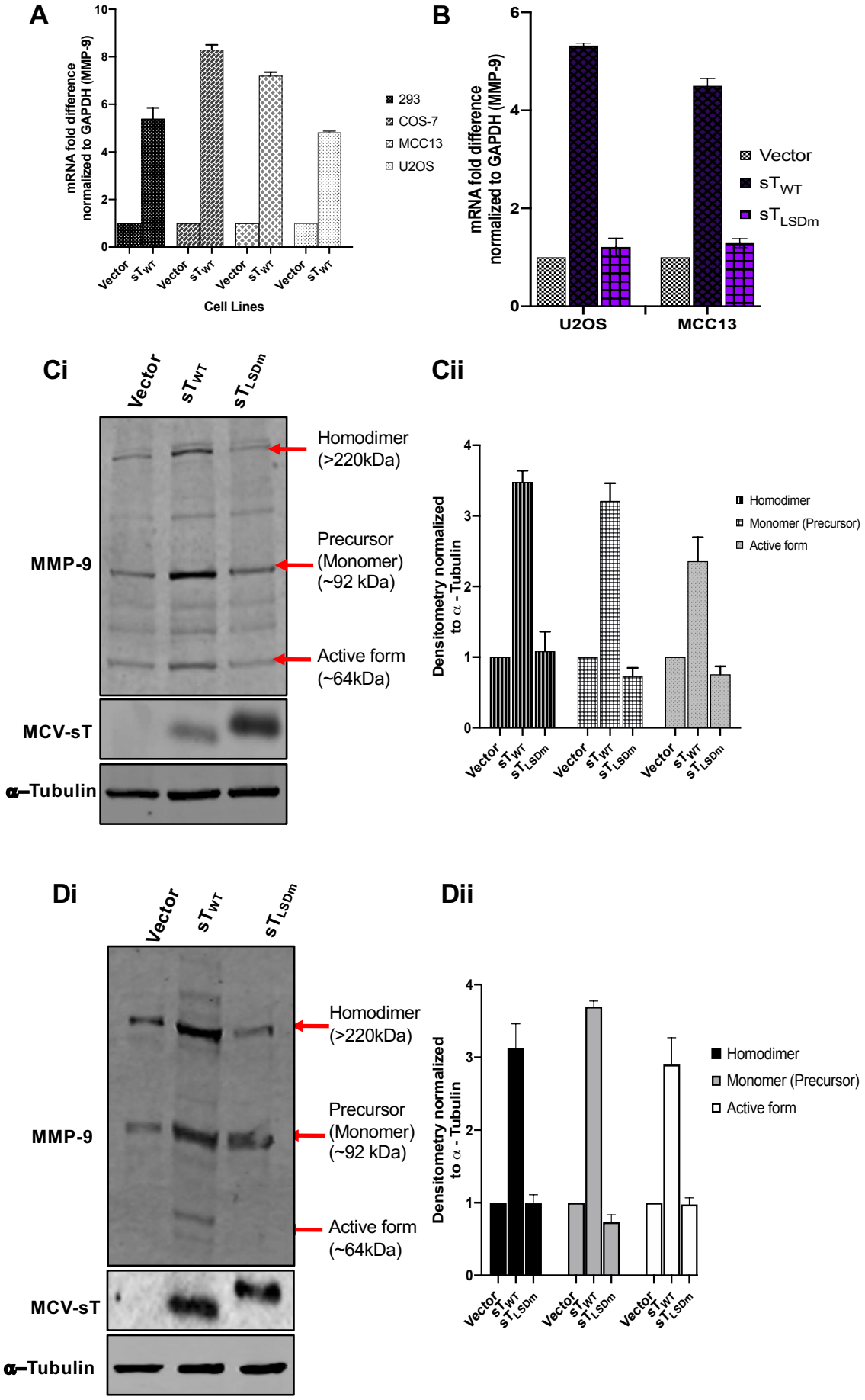
A
mRNA fold difference normalized to GAPDH (MMP-9)
293
COS-7
MCC13
U2OS
Vector
sTWT
Cell Lines
B
mRNA fold difference normalized to GAPDH (MMP-9)
Vector
sTWT
sTLSDm
U2OS
MCC13
Ci
Vector
sTWT
sTLSDm
Homodimer (>220kDa)
Precursor (Monomer) (~92 kDa)
Active form (~64kDa)
MMP-9
MCV-sT
α–Tubulin
Cii
Densitometry normalized to α - Tubulin
Homodimer
Monomer (Precursor)
Active form
Di
Vector
sTWT
sTLSDm
Homodimer (>220kDa)
Precursor (Monomer) (~92 kDa)
Active form (~64kDa)
MMP-9
MCV-sT
α–Tubulin
Dii
Densitometry normalized to α - Tubulin
Homodimer
Monomer (Precursor)
Active form

FIG 4

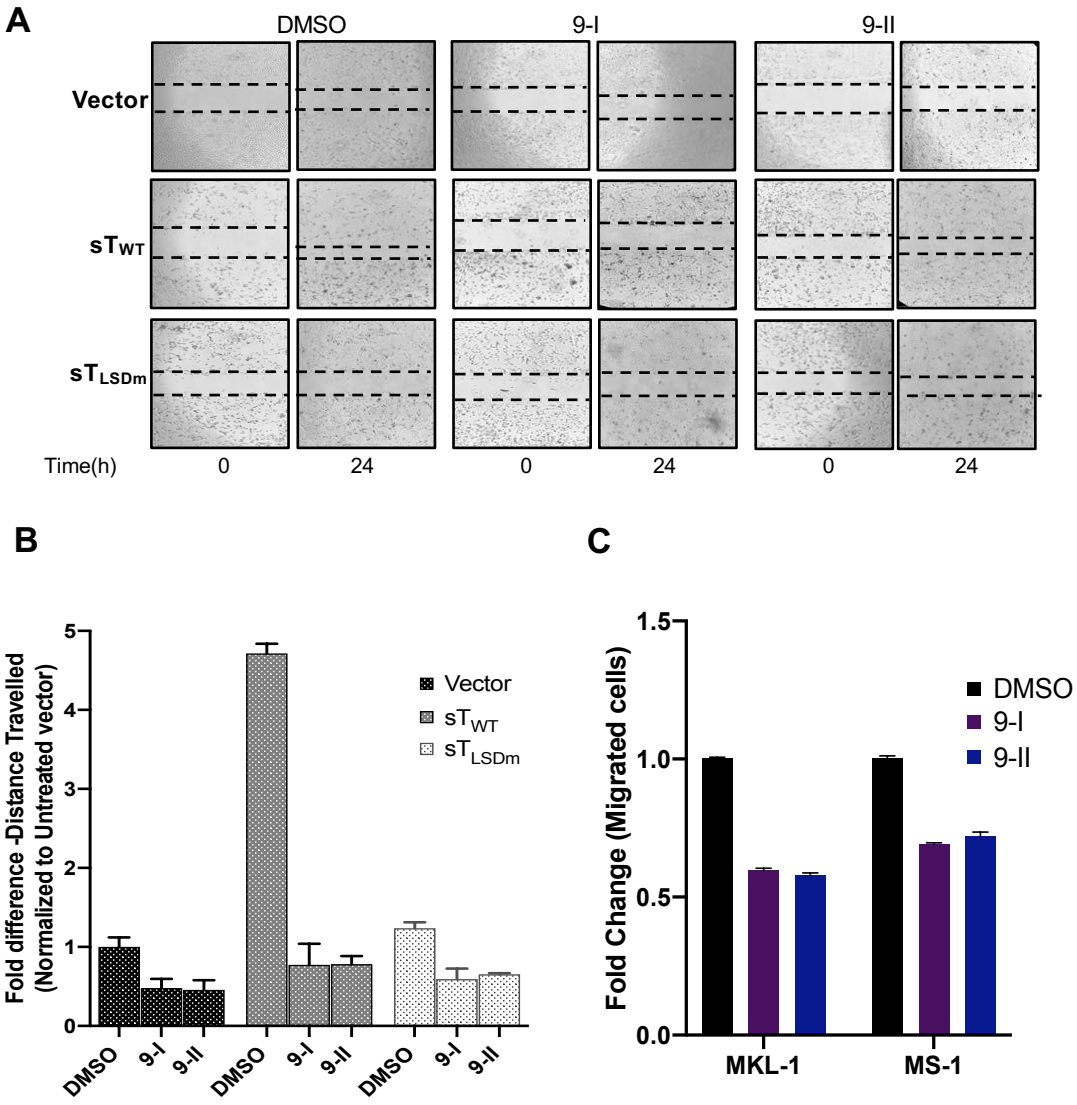
A
DMSO
9-I
9-II
Vector
sTWT
sTLSDm
Time(h)
0
24
0
24
0
24
B
Fold difference -Distance Travelled
(Normalized to Untreated vector)
Vector
sTWT
sTLSDm
DMSO
9-I
9-II
C
Fold Change (Migrated cells)
DMSO
9-I
9-II
MKL-1
MS-1

FIG 5

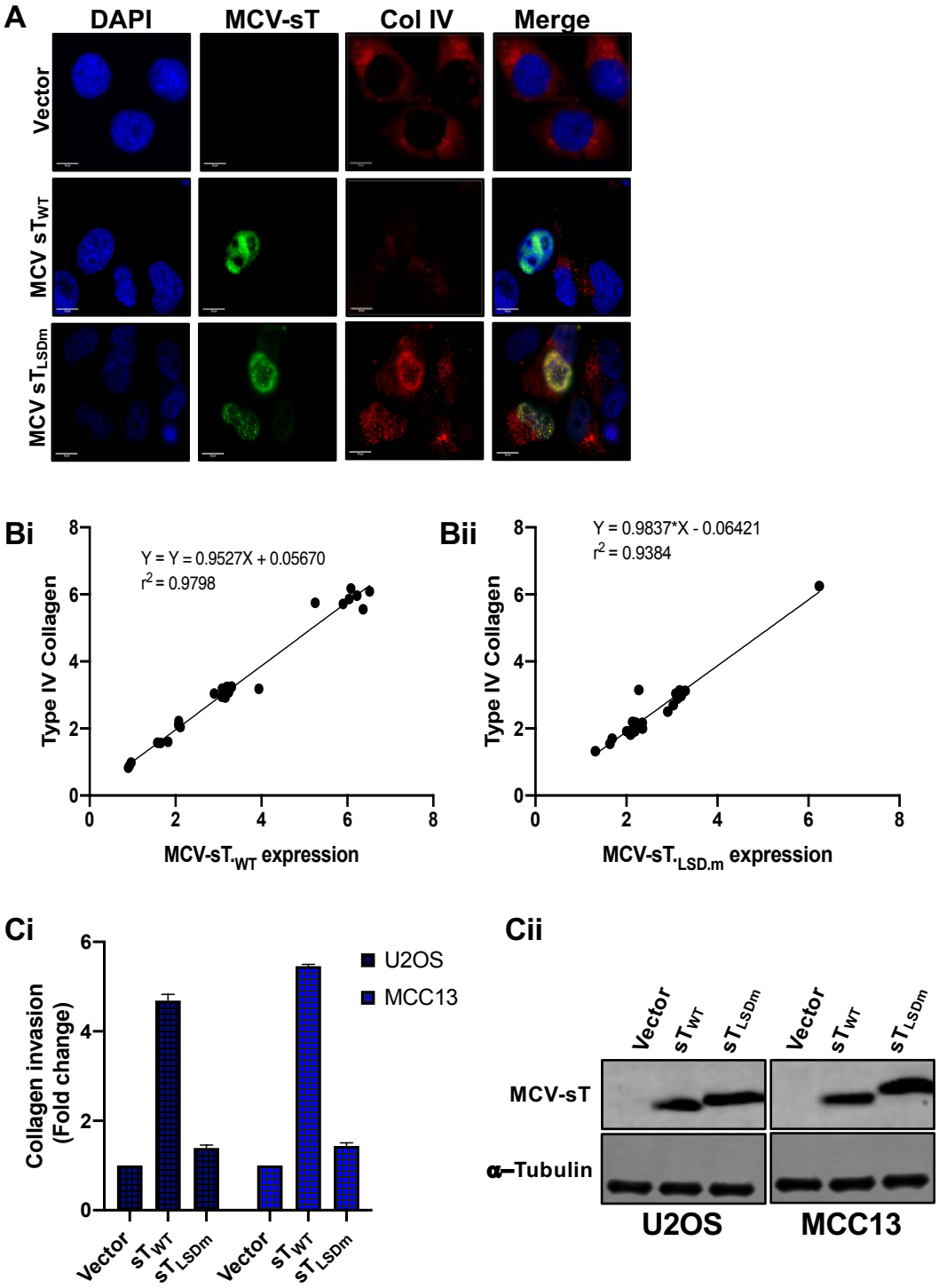
A
DAPI
MCV-sT
Col IV
Merge
Vector
MCV sT$_{WT}$
MCV sT$_{LSDm}$
Bi
Y = Y = 0.9527X + 0.05670
r^2 = 0.9798
Type IV Collagen
MCV-sT.$_{WT}$ expression
Bii
Y = 0.9837*X - 0.06421
r^2 = 0.9384
Type IV Collagen
MCV-sT.$_{LSD.m}$ expression
Ci
Collagen invasion (Fold change)
U2OS
MCC13
Vector
sT$_{WT}$
sT$_{LSDm}$
Cii
MCV-sT
α-Tubulin
U2OS
MCC13

FIG 6

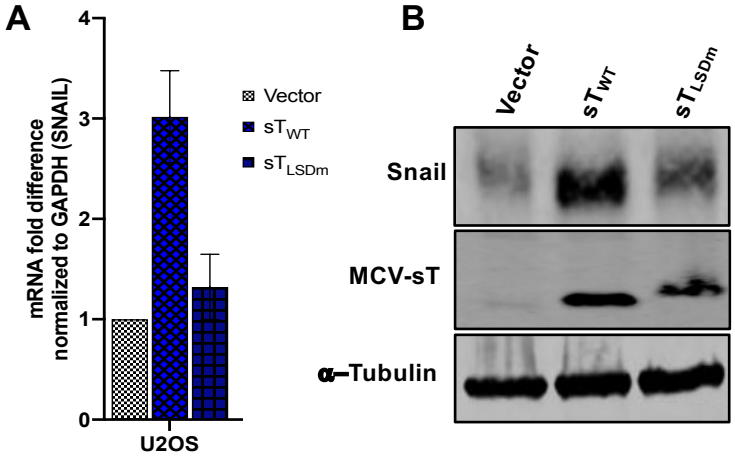
A
mRNA fold difference
normalized to GAPDH (SNAIL)
4
3
2
1
0
U2OS
Vector
sT WT
sT LSDm
B
Vector
sT WT
sT LSDm
Snail
MCV-sT
α–Tubulin